Electronic Supplementary Material (ESI) for Journal of Materials Chemistry A.

Supporting Information

Highly reversible zinc metal anodes enabled by three-dimensional silver host for aqueous batteries

Ruifang Xue[1], Jingyi Kong[1], Ying Wu[1], Yangyang Wang[1], Xiangyi Kong[1], Min Gong[1], Liang Zhang[1], Xiang Lin[1], Dongrui Wang* [1,2]

[1] Department of Chemistry and Chemical Engineering, School of Chemistry and Biological Engineering, University of Science and Technology Beijing, Beijing 100083, China

[2] Beijing Key Laboratory for Bioengineering and Sensing Technology, University of Science and Technology Beijing, Beijing 100083, China

*Corresponding Author, wangdr@ustb.edu.cn

Materials and Methods

Materials

Ag meshes with different mesh numbers (#30, #100, #180) woven from Ag wires (99.99 wt%, 0.05 mm in diameter) were purchased from Hebei Zhanmo Metals (China). Zn foil (99.9 wt%, 0.1 mm in thickness) and carbon cloth (CC) were from Tianjin Annuohe Energy Technology (China). Cu foam (99.9 wt%, 1.5 mm in thickness), Ti foil (0.02 mm in thickness), $LiFePO_4$ (LFP) powders, Ketjen Black (KB) conductive carbon and polyvinylidene fluoride (PVDF) were obtained from Shenzhen Kejing Star Technology Company. $ZnSO_4 \cdot 7H_2O$ (AR), Na_2SO_4 (AR), LiCl (AR) were purchased from Sigma Aldrich. N-methyl-2-pyrrolidone (NMP) was from Shanghai Aladdin Biochemical Technology. Deionized water with the resistivity of 18.2 MΩ·cm was obtained from Milli-Q water purification system.

Preparation of asymmetric cells

The Ag meshes were firstly washed with ethanol to remove the surface contaminants and punched into round disks with the diameter of 16 mm after drying. CR2032-type coin cells were assembled using Ag meshes as the working electrode and Zn foils as the counter and reference electrodes. Glass microfiber membrane (Whatmann) was used as the separator and the aqueous solution containing 2 M $ZnSO_4$ was selected as the electrolyte. Control cells were assembled by using copper foam and CC as the working electrode.

Preparation of 3D Zn anodes (Zn@a-Ag mesh)

The asymmetric cells with Ag mesh #180 as the working electrode were galvanostatically cycled for 3 cycles under a current density of 2 mA/cm^2 with a discharged capacity of 1 mAh/cm^2. Then the cells were discharged at 5 mA/cm^2 for 0.4 h to electroplate Zn onto the surface-alloyed Ag meshes (a-

Ag mesh). Finally, the cells were carefully disassembled and the Zn@a-Ag mesh anodes were thoroughly washed with deionized water and dried under vacuum.

Preparation of hybrid-ion batteries

The cathodes were prepared by coating the slurry of LFP, KB and PVDF with a mass ratio of 70:20:10 on Ti foil and dried at 80 °C under vacuum for 12 h. Then the cathodes were cut into round disks with the diameter of 16 mm. The mass loading of LFP was about 3 mg/cm^2. Full cells were then assembled using such LFP cathodes to pair with the above-mentioned 3D Zn anodes with the areal capacity of about 2 mAh/cm^2. The aqueous solution containing 2 M $ZnSO_4$ and 1 M LiCl was used as the electrolyte. Full cells by using Zn foil anode were also assembled and tested as control.

Electrochemical measurements

For the testing of Coulombic efficiencies (CE), asymmetric cells were galvanostatically cycled under varying current densities (1-10 mA/cm^2) and capacities (0.5-15 mAh/cm^2) with the stripping cut-off voltage of 0.5 V. For the hybrid-ion battery cycling tests, the full cells were charged and discharged under various current densities within 0.85-1.6 V. All the cycling tests were performed on a Neware battery testing system at room temperature. Cyclic voltammetry (CV), linear sweep voltammetry (LSV), and Tafel curves were measured on an electrochemical workstation (CHI 660E). LSV measurements were carried out in a three-electrode system, wherein the Ag meshes, Zn foil and Ag/AgCl in saturated KCl solution were used as working, counter and reference electrodes, respectively. The electrolyte was 2 M Na_2SO_4 solution and the scan rate was 5 mV/s. Electrochemical impedance spectroscopy (EIS) of the full cells were also tested by using the electrochemical workstation over the frequency range of 10^{-2}-10^5 Hz.

Material Characterizations

Scanning electron microscopy (SEM) observation was carried out using SU8010 (Hitachi, Japan) at an accelerating voltage of 5 kV. X-ray diffraction (XRD) patterns were recorded on a diffractometer (Panalytical Empyrean series 3). The measurements were performed at room temperature with Cu Kα radiation (λ = 1.541 Å). All *ex-situ* studies with SEM and XRD were conducted after the tested electrodes were collected and thoroughly washed with deionized water.

Table S1. Comparison of Ag meshes, Cu foam, and carbon cloth in physical properties.

	Ag mesh (#180)	Ag mesh (#100)	Ag mesh (#30)	Cu foam	Carbon cloth
Pore diameter (μm)	100	150	700	-	-
Areal density (mg cm^{-2})	29	38	47	38	12
Thickness (μm)	105	130	300	1500	250
Theoretical conductivity (S/m, 20 °C)	6.30×10^7	6.30×10^7	6.30×10^7	5.96×10^7	2.0×10^5

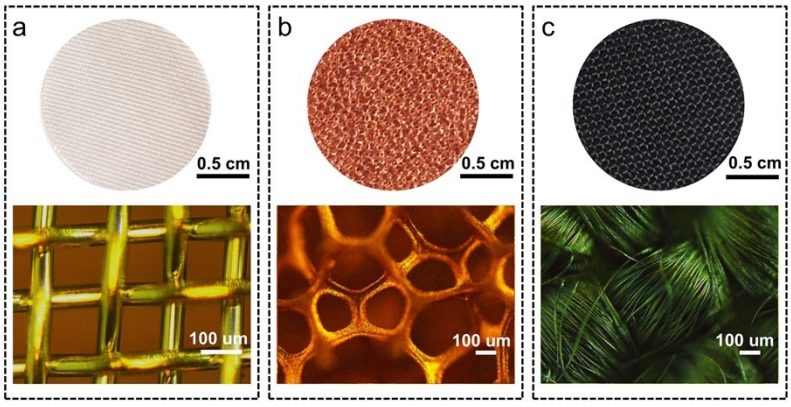

Figure S1. Typical optical and SEM images of the Ag mesh (#180), Cu foam, and carbon cloth.

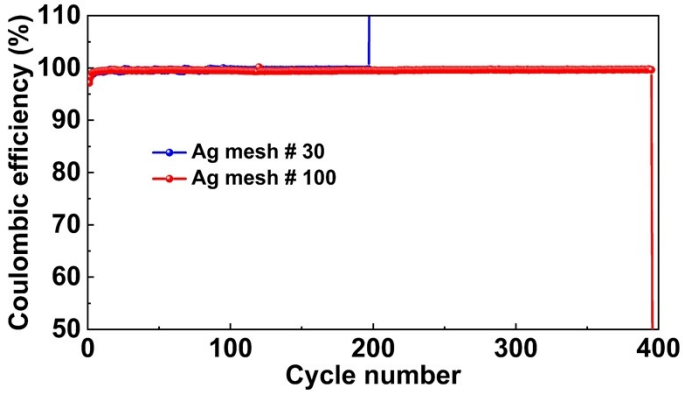

Figure S2. Coulombic efficiency of asymmetric Ag mesh//Zn foil cells cycling at 5 mA/cm^2 with a determined capacity of 1.0 mAh/cm^2.

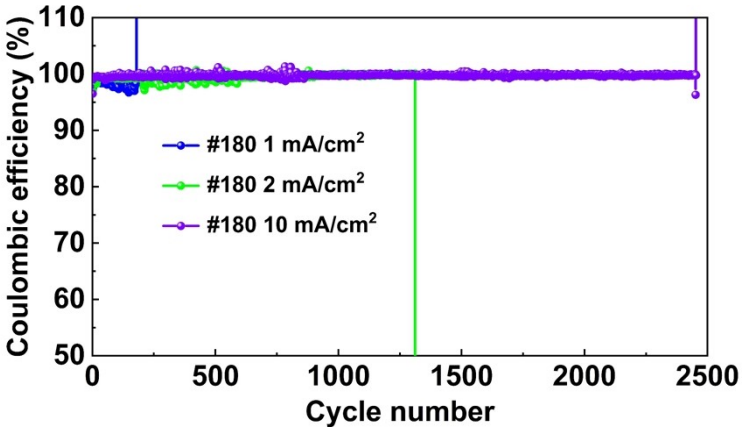

Figure S3. Coulombic efficiency of Ag mesh (#180)//Zn foil cells cycling at different current densities with a determined capacity of 1.0 mAh/cm^2.

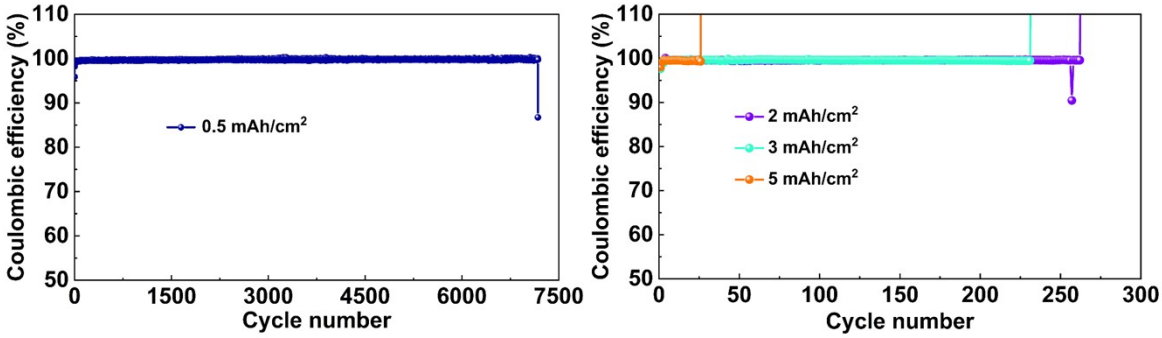

Figure S4. Coulombic efficiency of Ag mesh (#180) //Zn foil cells cycling at 5 mA/cm^2 with different capacities.

Figure S5. Photographs of the CC//Zn cell after 500 cycles (left) and the Ag mesh//Zn cell after 2000 cycles (right).

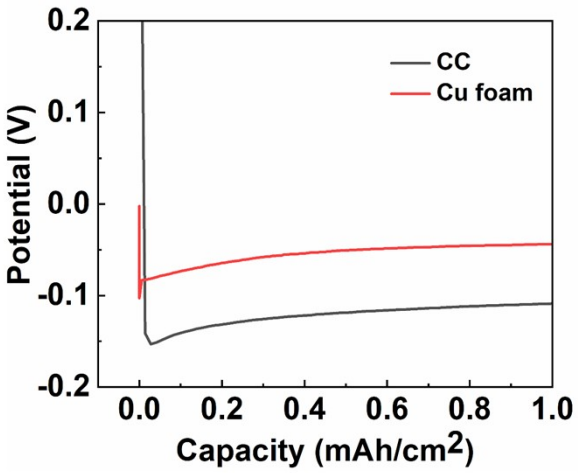

Figure S6. Galvanostatic plating curves of Cu foam and CC at the current of 5 mA/cm^2.

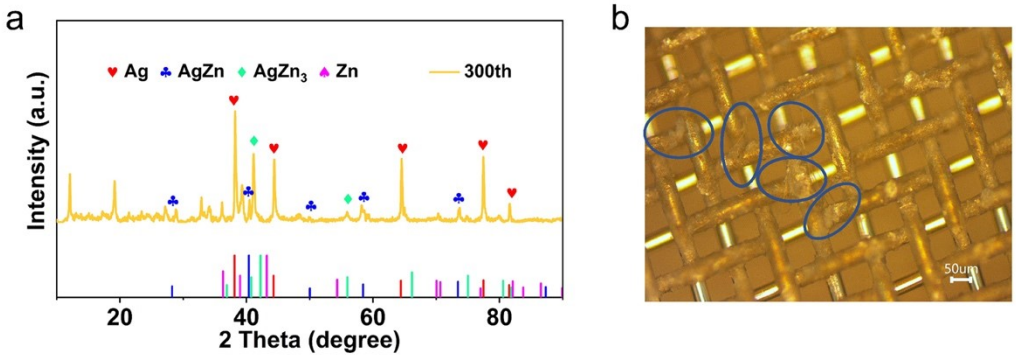

Figure S7. (a) *Ex-situ* XRD pattern and (b) optical image of the a-Ag mesh after 300 cycles of Zn plating/stripping at 2 mA/cm^2 and 1 mAh/cm^2. The circles in (b) denote the fragments of the glass fiber separator that are strongly adhered on the a-Ag mesh.

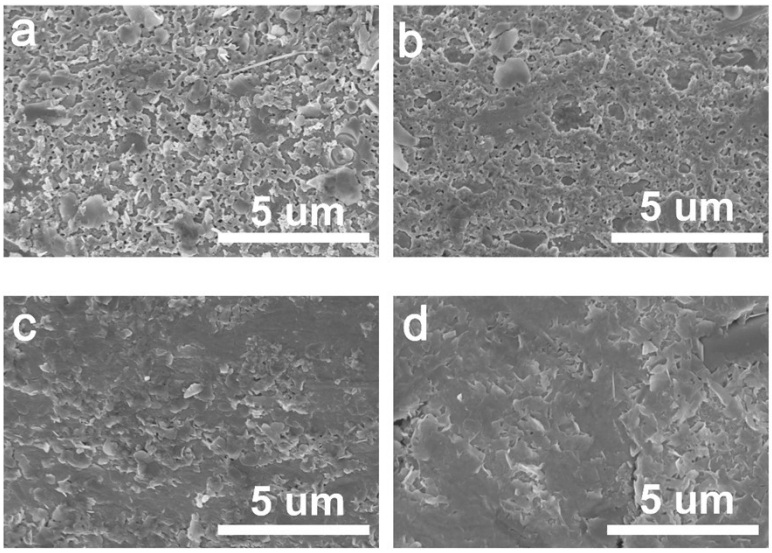

Figure S8. SEM images of the Zn@a-Ag anode in different time intervals during the first plating cycle at 5 mA/cm^2. Panels a-d correspond deposition time of 5 s, 10 s, 6 min and 10 min, respectively.

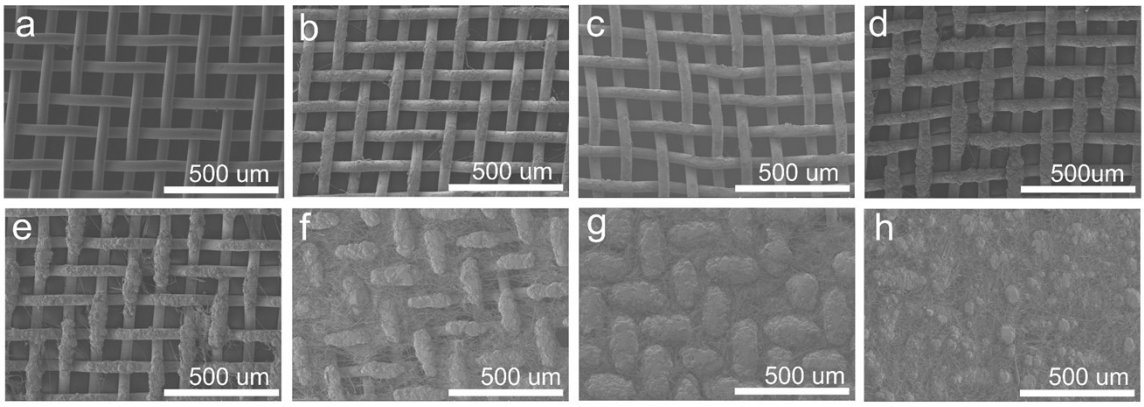

Figure S9. SEM images of Ag mesh (a) and the morphologies after Zn deposits on a-Ag mesh at a current density of 5 mA/cm^2 with different Zn capacities 0.5 (b), 1.0 (c), 2.0 (d), 3.0 (e), 5.0 (f), 10.0 (g), 15.0 (h) mA h/cm^2.

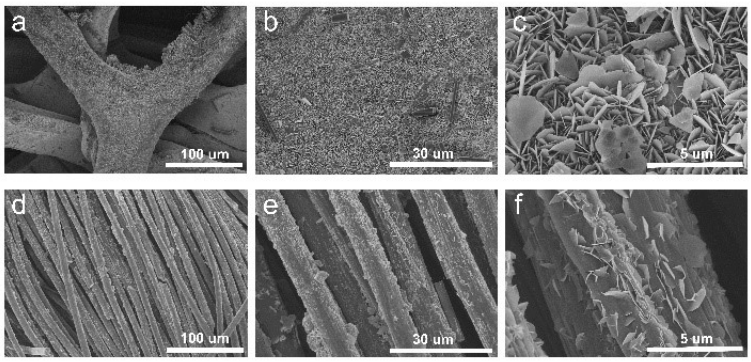

Figure S10. SEM images of electrodeposited Zn on (a-c) Cu foam and (d-f) CC at 5 mA/cm^2 with the capacity of 1 mAh/cm^2.

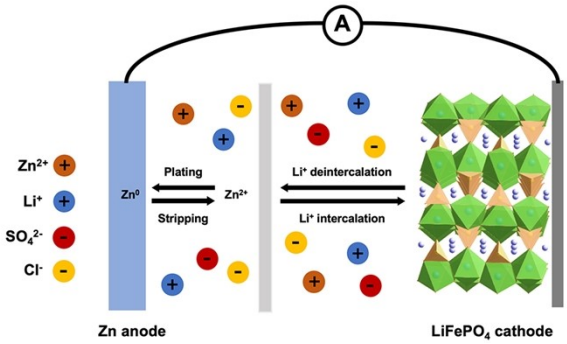

Figure S11. Schemetic illustration for the mechanism of the aqeous hybrid ion battery using $LiFePO_4$ as the cathode material and metallic Zn as the anode.

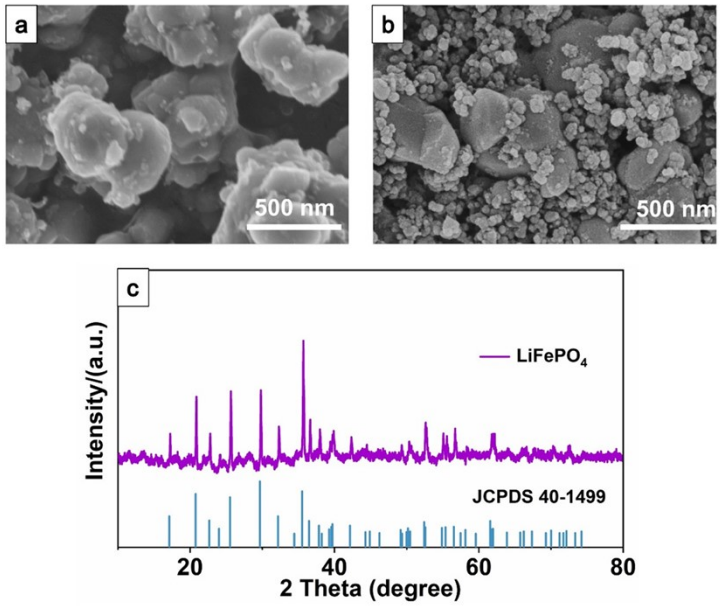

Figure S12. SEM images of $LiFePO_4$ before (a) and after (b) mixed with KB and PVDF. (c) XRD pattern of the $LiFePO_4$.

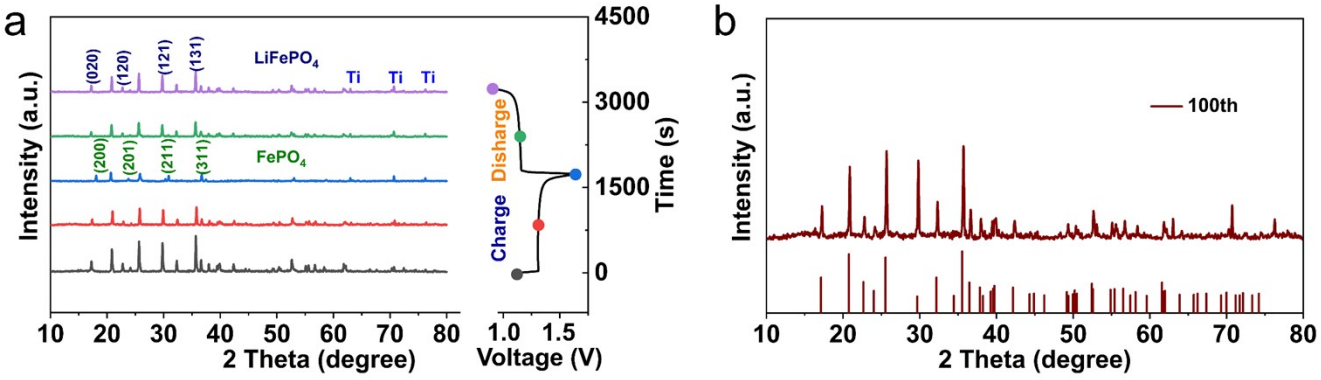

Figure S13. *Ex-situ* XRD patterns of the $LiFePO_4$ cathode collected from Zn@a-Ag mesh//LFP batteries at different electrochemical states at 0.5 mA/cm^2 during the first charge/discharge cycle (a) and after the 100th charging/discharing cycle (b).

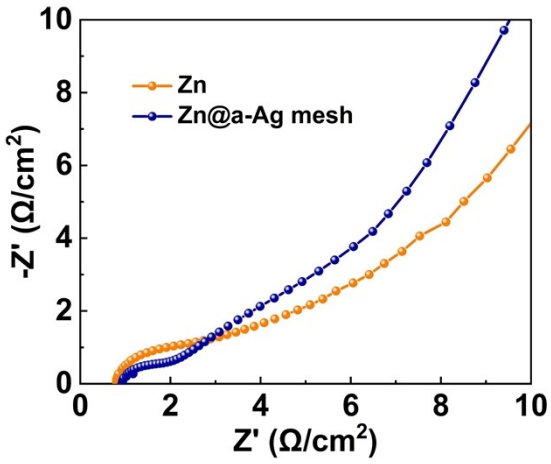

Figure S14. Nyquist plots of as-assembled Zn@a-Ag mesh//LFP and Zn//LFP batteries.

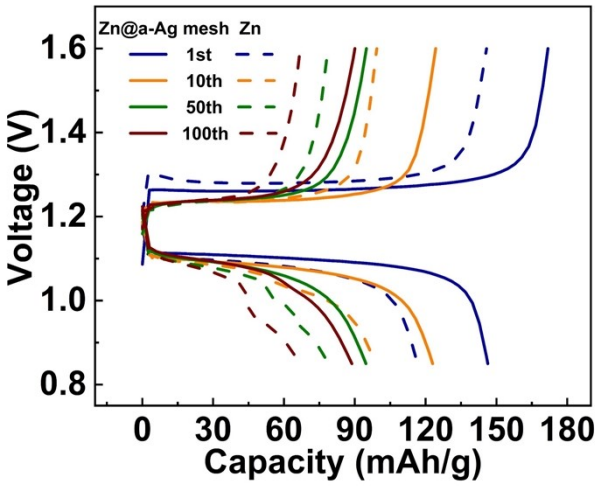

Figure S15. Galvanostatic charge/discharge curves of Zn@a-Ag mesh//LFP (solid lines) and Zn//LFP (dash lines) at various cycle numbers under the cycling current of 0.5 mA/cm^2.

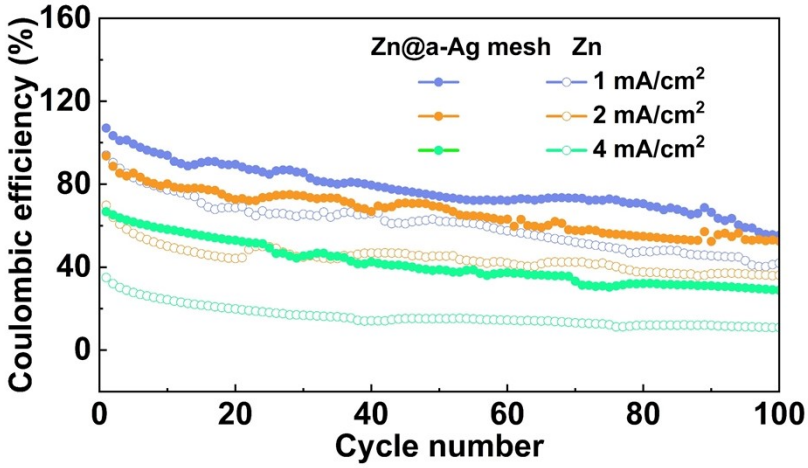

Figure S16. Cycling performance of Zn@a-Ag mesh//LFP and Zn//LFP batteries at 1, 2 and 4 mA/cm^2 for 100 cycles.

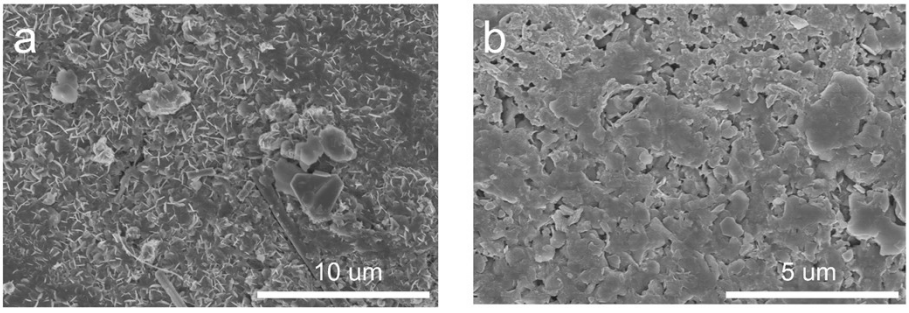

Figure S17. SEM images of Zn foil (a) and Zn@a-Ag mesh anode (b) in hybrid full cells after charging/discharging at 0.5 mA/cm^2 for 100 cycles.

Table S2. A survey of cyclic performance of various Zn-based asymmetric cells using 3D hosts or Ag-modified current collectors via the "reservoir-free" galvanostatic plating/stripping protocol.

Host	Electrode area (cm^2)	Electrolyte	Current density (mA/cm^{-2})	Plated Zn per cycle (mAh/cm^{-2})	CE (%)	Life cycle	Cumulative capacity of transported Zn[a] (mAh)	Ref.
a-Ag mesh	2.0	2 M $ZnSO_4$	1	1	98.3	179	358	This work
			2	1	99.5	1312	2624	
			5	1	99.5	2275	4550	
			10	1	99.8	2452	4904	
			5	0.5	99.8	7175	7175	
			5	2	99.5	262	1048	
			5	3	99.6	231	1386	
			5	5	99.4	26	260	
Porous copper skeleton	1.0	2 M $ZnSO_4$	1	2	99.53	66	132	[1]
CNT arrays on carbon cloth	Unknown	2 M $ZnSO_4$	2	2	~96	30	120 [b]	[2]
			5	2	~97.9	30		
Zn@ZnO-3D	1.77	2 M $ZnSO_4$ + 0.1 M $MnSO_4$	2	0.5	99.55	300	265.5	[3]
Cu foam	1.13	2 M $ZnSO_4$	5	1	-	300	339	[4]
Ni foam			5	1	-	300		
AgNPs@Carbon	Unknown	1 M	5	2	99.5	800	3200 [b]	[5]

Cloth		$Zn(CF_3SO_3)_2$						
ZIF-8@Ni grid	Unknown	2 M $ZnSO_4$	20	3	99.5	200	1200 [b]	6
MXene paper	1.5	2 M $ZnSO_4$	1	1	94.13	400	600	7
NOCA@Cu foam	Unknown	2 M $ZnSO_4$	1	1	95.7	350	700 [b]	8
Cu foam	1.13	2 M $ZnSO_4$	1	1	-	~55	~65	9
Cu@Stainless steel foil	0.79	3 M $ZnSO_4$ + 0.1 M $MnSO_4$	1	1	99.4	700	553	10
			10	1	99.7	3000	2370	
Ag@Stainless steel foil			10	1	99.6	2400	1896	
			10	3	98.6	280	664	
AgNWs@Ti foil	Unknown	2 M $ZnSO_4$	2	1	97.79	300	600 [b]	11

[a] The value was calculated as the product of the amount of Zn plated in each cycle, the cycle life and the electrode area.

[b] Estimated value, assuming that the area of tested electrodes in coin cells is as large as 2.0 cm^2.

References

1. Z. Kang, C. Wu, L. Dong, W. Liu, J. Mou, J. Zhang, Z. Chang, B. Jiang, G. Wang, F. Kang and C. Xu, *ACS Sustainable Chemistry & Engineering*, 2019, **7**, 3364-3371.
2. Y. Zeng, X. Zhang, R. Qin, X. Liu, P. Fang, D. Zheng, Y. Tong and X. Lu, *Advanced Materials*, 2019, **31**, 1903675.
3. X. Xie, S. Liang, J. Gao, S. Guo, J. Guo, C. Wang, G. Xu, X. Wu, G. Chen and J. Zhou, *Energy & Environmental Science*, 2020, **13**, 503-510.
4. X. Shi, G. Xu, S. Liang, C. Li, S. Guo, X. Xie, X. Ma and J. Zhou, *ACS Sustainable Chemistry & Engineering*, 2019, **7**, 17737-17746.
5. T. Chen, Y. Wang, Y. Yang, F. Huang, M. Zhu, B. T. W. Ang and J. M. Xue, *Advanced Functional Materials*, 2021, **31**, 2101607.
6. Z. Wang, J. Huang, Z. Guo, X. Dong, Y. Liu, Y. Wang and Y. Xia, *Joule*, 2019, **3**, 1289-1300.
7. Y. Tian, Y. An, C. Wei, B. Xi, S. Xiong, J. Feng and Y. Qian, *ACS Nano*, 2019, **13**, 11676-11685.
8. Y. An, Y. Tian, Y. Li, C. Wei, Y. Tao, Y. Liu, B. Xi, S. Xiong, J. Feng and Y. Qian, *Chemical Engineering Journal*, 2020, **400**, 125843.
9. C. Li, X. Shi, S. Liang, X. Ma, M. Han, X. Wu and J. Zhou, *Chemical Engineering Journal*, 2020, **379**, 122248.
10. Y. Zhang, G. Wang, F. Yu, G. Xu, Z. Li, M. Zhu, Z. Yue, M. Wu, H.-K. Liu, S.-X. Dou and C. Wu, *Chemical Engineering Journal*, 2021, **416**, 128062.
11. Z. Li, H. Wang, Y. Zhong, L. Yuan, Y. Huang and Z. Li, *ACS Applied Materials & Interfaces*, 2022, **14**, 9097-9105.